Magnetic and transport properties of iron-platinum arsenide $Ca_{10}(Pt_{4-\delta}As_8)(Fe_{2-x}Pt_xAs_2)_5$ single crystal

Qing-Ping Ding,[1,2] Yuji Tsuchiya,[1] Shyam Mohan,[1] Toshihiro Taen,[1] Yasuyuki Nakajima,[1,2] and Tsuyoshi Tamegai[1,2]

[1]*Department of Applied Physics, The University of Tokyo, 7-3-1 Hongo, Bunkyo-ku, Tokyo 113-8656, Japan*

[2]*JST, Transformative Research-Project on Iron Pnictides (TRIP), 7-3-1 Hongo, Bunkyo-ku, Tokyo 113-8656, Japan*

(Received 25 December 2011; revised manuscript received 21 February 2012; published 14 March 2012)

We report superconducting properties of single crystalline $Ca_{10}(Pt_{4-\delta}As_8)(Fe_{2-x}Pt_xAs_2)_5$ by x-ray diffraction, magnetization, resistivity, and magneto-optical imaging measurements. The magnetization measurements reveal a fish-tail hysteresis loop and relatively high critical current density $J_c \sim 0.8 \times 10^5$ A/cm^2 at low temperatures. The exponential temperature dependence of J_c, which arises from the nonlinear effective flux-creep activation energy, has been observed. The upper critical field determined by resistive transition shows a relatively large anisotropy. The magneto-optical images reveal a homogenous current flow within the crystal.

DOI: 10.1103/PhysRevB.85.104512 PACS number(s): 74.25.Ha, 74.25.Sv, 74.62.Bf

I. INTRODUCTION

A series of iron-based superconductors has been synthesized after the discovery of superconductivity in oxypnictide $LaFeAsO_{1-x}F_x$ (1111) with a critical temperature $T_c \sim 26$ K.[1–18] Layers of Fe tetrahedrally coordinated by As or chalcogens are common features in these materials, which is similar to the CuO_2 layer in high-T_c cuprates. In iron-based superconductors, blocking layers with alkali, alkali-earth, rare-earth oxides, alkali-earth fluorides, and complex metal oxides are alternatively stacked with Fe-As layers.[1–9,11–18] The ionic chemical bonds which appear within the blocking layers make them insulating. Recently, intermetallic Pt-As layers were introduced as new blocking layers since Pt is very flexible and can form arsenides with different coordinations.[19–23] Two structures of iron-platinum arsenides with the composition $Ca_{10}(Pt_3As_8)(Fe_{2-x}Pt_xAs_2)_5$ (10-3-8) and $Ca_{10}(Pt_4As_8)(Fe_{2-x}Pt_xAs_2)_5$ (10-4-8) with T_c of ~13 K and above 30 K, respectively, have been identified.[19–22] Although "high-quality" single crystals have been reported by several groups, the homogeneity of the superconducting states has not yet been investigated. The upper critical field (H_{c2}) is an important parameter in superconductors. Most iron-based superconductors show relatively weak anisotropy of H_{c2}. In particular, H_{c2} in Fe(Te,Se) is almost isotropic at low temperatures.[24] In $Ba(Fe,Co)_2As_2$, the anisotropy is also very small.[25,26] This small anisotropy is a typical difference between most iron-based superconductors and cuprate superconductors. Bearing a different structure from other iron-pnictides, the degree of the anisotropy in iron-platinum arsenides is an interesting topic. Critical current density is another eye-catching and important parameter of superconductors. The ability to carry an electrical current without dissipation enables their use in devices such as high power transmission lines, high field magnets, compact high quality filters, and so on. The exploration of higher critical current density not only gives the answer needed for practical applications, but also sheds light on the fundamental properties of the superconducting state itself. The above-mentioned curiosities constitute the motivations of our present study.

In this paper, we report on the synthesis and characterizations of high-quality $Ca_{10}(Pt_{4-\delta}As_8)(Fe_{2-x}Pt_xAs_2)_5$ single crystals. The characterization through x-ray diffraction, Energy-dispersive X-ray spectroscopy (EDX), magnetization, and resistivity measurements are discussed. We also adopted magneto-optical (MO) imaging techniques to check the homogeneity of the prepared crystal.

II. EXPERIMENTS

Ca chips (Rare Metallic, 99.5%), As pieces (Furukawa Denshi, 99.99999%), Pt chips (Furuya Metal, 99.95%), and FeAs powder were used as starting materials to prepare $Ca_{10}(Pt_{4-\delta}As_8)(Fe_{2-x}Pt_xAs_2)_5$ single crystals. FeAs was prepared by placing stoichiometric amounts of As pieces (Furukawa Denshi, 99.99999%) and Fe powder (Kojundo Chemical Laboratory, 99%) in an evacuated quartz tube and reacting them at 1065 °C for 10 h after heating at 700 °C for 6 h. The mixture of 2 g with a ratio of Ca: Fe: Pt: As = 15 : 16 : 8 : 30 was loaded into an alumina crucible (inner diameter 12 mm) and sealed in an evacuated quartz tube (inner diameter 18 mm). The whole assembly was heated up to 1000 °C for 72 h after heating at 700 °C for 5 h, followed by cooling down to 800 °C at a rate of 3 °C/h. Then the furnace was switched off and cooled to room temperature naturally.

The phase identification of the sample was carried out by means of x-ray diffraction (M18XHF, MAC Science) with Cu-$K\alpha$ radiation generated at 40 kV and 350 mA. The chemical composition of the crystal was confirmed by EDX (S-4300, Hitachi High-Technologies equipped with EMAX x-act, Horiba). Bulk magnetization is measured by a superconducting quantum interference device (SQUID) magnetometer (MPMS-5XL, Quantum Design). Resistivity measurements were performed in the sample chamber of a SQUID magnetometer by the four-probe method with silver paste for electrical contacts. MO imaging was employed for local magnetic characterization. A Bi-substituted iron-garnet indicator film was placed in direct contact with the sample, and the whole assembly was attached to the cold finger of a He-flow cryostat (Microstat-HR, Oxford Instruments). MO images were acquired by using a cooled charged-coupled device (CCD) camera with 12-bit resolution (ORCA-ER, Hamamatsu). To enhance the visibility of the local magnetic induction and eliminate the signals from the impurity phases and scratches in the garnet film a differential imaging technique was adopted.[27,28]

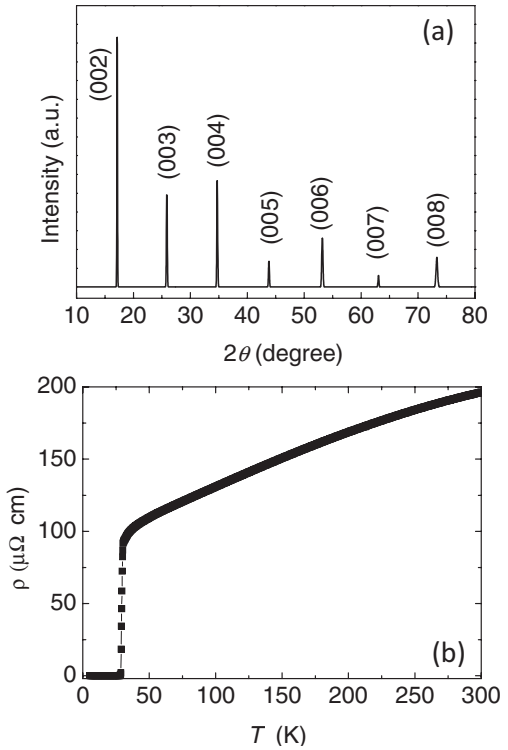

FIG. 1. (a) X-ray diffraction pattern of as-prepared single crystal. (b) Temperature dependence of in-plane resistivity of $Ca_{10}(Pt_{4-\delta}As_8)(Fe_{2-x}Pt_xAs_2)_5$ single crystal.

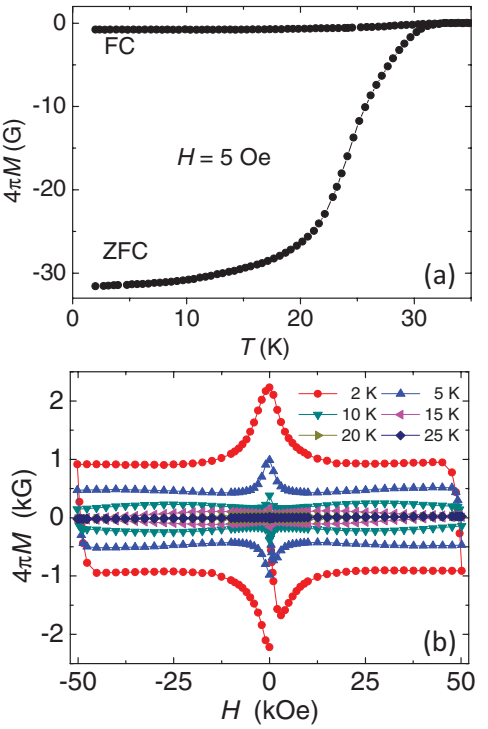

FIG. 2. (Color online) (a) Temperature dependence of ZFC and FC magnetization in $Ca_{10}(Pt_{4-\delta}As_8)(Fe_{2-x}Pt_xAs_2)_5$ measured at 5 Oe. (b) Magnetic field dependence of magnetization in $Ca_{10}(Pt_{4-\delta}As_8)(Fe_{2-x}Pt_xAs_2)_5$ at different temperatures ranging from 2 to 25 K.

III. RESULTS AND DISCUSSIONS

Figure 1(a) shows the x-ray diffraction pattern of an as-prepared single crystal. Only 00*l* peaks are observed, and the *c*-axis lattice constant is calculated as 1.0343 nm, which is a little smaller than that of Refs. 20–22. The chemical composition of the crystal determined by EDX analyses is $Ca_{10}(Pt_{4-\delta}As_8)(Fe_{1.96}Pt_{0.04}As_2)_5$ with $\delta = 0.49$ based on the ratio of each element.

Figure 1(b) shows the temperature dependence of the resistivity of the $Ca_{10}(Pt_{4-\delta}As_8)(Fe_{2-x}Pt_xAs_2)_5$ single crystal. The resistivity at room temperature is relatively low with 200 $\mu\Omega$ cm, and shows a metallic behavior in the normal state. A sharp drop in resistivity was observed starting from 30.3 K, which indicates the onset of superconductivity. The zero resistivity occurs at 28.7 K and the transition width is 1.6 K. The residual resistivity ratio (RRR) $\rho(300\,\mathrm{K})/\rho(T_c^{\mathrm{onset}})$ is 2.15. Relatively large $\rho(T_c^{\mathrm{onset}})$ and small RRR may reflect the presence of Pt ions in FeAs layers as suggested by the authors of Refs. 19–22.

The temperature dependences of zero-field-cooled (ZFC) and field-cooled (FC) magnetizations at 5 Oe of the $Ca_{10}(Pt_{4-\delta}As_8)(Fe_{2-x}Pt_xAs_2)_5$ single crystal are shown in Fig. 2(a). The sample shows the onset of diamagnetism at $T_c \sim 33$ K. Figure 2(b) shows the magnetization as a function of field at several temperatures ranging from 2 to 25 K.

From the magnetization hysteresis loops, we can evaluate global critical current density J_c for a single crystal using the Bean's model with the assumption of field-independent J_c. According to the Bean model,[29] J_c [A/cm^2] is given by

$$J_c = 20\frac{\Delta M}{a(1-a/3b)}. \quad (1)$$

where ΔM [emu/cc] is M_{down}-M_{up}, M_{up} and M_{down} are the magnetization when sweeping the field up and down, respectively, a [cm] and b [cm] are sample widths ($a < b$). Figure 3(a) shows the field dependences of calculated J_c from the data shown in Fig. 2(b) using Eq. (1) and sample dimensions $a \sim 800$ μm and $b \sim 1190$ μm.

A pronounced nonmonotonic field dependence of J_c with a broad maximum, fish-tail effect, is clearly observed at temperatures higher than 10 K as shown in Fig. 2(b). The same effect is believed to exist below 10 K with a much higher peak field above 50 kOe. The fish-tail effect is more clearly seen in the field dependence of J_c as shown in Fig. 3(a). First of all, we define the fish-tail effect in the present context. This name was invented in the study of high temperature cuprate superconductors, which often showed a broad peak in the magnetic field dependence of the critical current density. Such a broad peak in J_c-H is ubiquitous among cuprate superconductors,[30,31] except for very anisotropic $Bi_2Sr_2CaCu_2O_{8+y}$ compounds.[32] It was also widely observed in iron-based superconductors except for some isovalently doped systems such as $BaFe_2(As,P)_2$ (Ref. 33), although some other reports on the same material demonstrate the presence of the fish-tail effect.[34] The fish-tail effect can be considered to be one special form of peak effects. Among many origins for the peak effect, some well-known examples are due to the

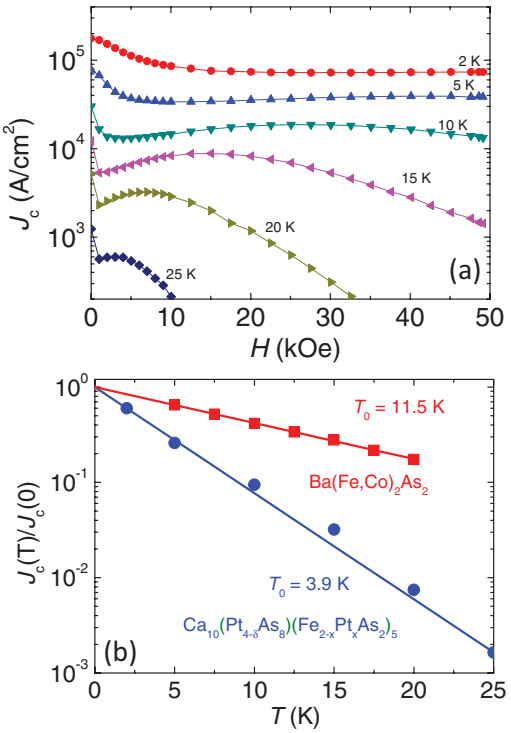

FIG. 3. (Color online) (a) Magnetic field dependence of critical current densities obtained from the M-H curves shown in Fig. 2(b). (b) Critical current density J_c relative to its value at absolute zero temperature, decreases roughly exponentially $\exp(-T/T_0)$, due to flux creep. With zero field, normalized J_c for the $Ca_{10}(Pt_{4-\delta}As_8)(Fe_{2-x}Pt_xAs_2)_5$ single crystal compared to that for $Ba(Fe,Co)_2As_2$ single crystals.

softening of the vortex lattice close to H_{c2} (Ref. 35), called synchronization, or the geometrical matching of the vortex system to the underlying periodicity of the pinning potential in the sample.[36] In most cases, the peak in J_c is rather sharp. In contrast to this, the fish-tail effect in the cuprate is, in general, defined by the broad peak in J_c-H characteristics. The mechanism for this phenomenon can be classified into two origins, namely static and dynamic origins. In the former case, regions with lower T_c in the sample turn into normal or close to normal, thus serving as pinning centers. Since the T_c of such weak superconducting regions is expected to have a broad distribution, the enhancement of J_c occurs in a broad magnetic field range. Another mechanism is related to the dynamics of the vortex system. In the collective creep theory, the creep exponent strongly depends on the size of the vortex bundle, which is a function of the magnetic field.[37] In a single vortex regime, the creep exponent is $\mu = 1/7$ and it crosses over to $3/2$ in the small bundle regime. A smaller μ corresponds to the faster motion of vortices, and hence the irreversible magnetization at the measuring time scale of the order of 1 s to 1min becomes small, resulting in an increase of J with magnetic field.[38] As the field is further increased, the creep exponent becomes $7/9$ in the large bundle regime and the vortex creep becomes faster and the increase in J_c with H would be weakened. However, the collective creep model is based on the elastic deformation of vortices. So, when the plastic deformations set in, the situation may change drastically. The elastic to plastic crossover scenario for the fish-tail effect is based on this kind of consideration. "Crossover from elastic to plastic" is the most plausible origin of the fish-tail in the $Ca_{10}(Pt_{4-\delta}As_8)(Fe_{2-x}Pt_xAs_2)_5$ and other iron-based superconductors. It is partly supported by the strong acceleration of vortex motion above the peak field as demonstrated in various iron-based superconductors including $Ba(Fe,Co)_2As_2$ (Refs. 25 and 39).

J_c calculated from the M-H curve is estimated to be 0.8×10^5 A/cm^2 at 5 K under zero field, which is smaller than that of the optimally doped $Ba(Fe_{1-x}Co_x)_2As_2$ single crystal, but similar to the $FeTe_{0.6}Se_{0.4}$ single crystal,[40] and still in the range for applications. J_c values in excess of 0.3×10^5 A/cm^2 are sustained up to 50 kOe at 5 K. One reason for the low J_c is that since $Ca_{10}(Pt_{4-\delta}As_8)(Fe_{2-x}Pt_xAs_2)_5$ is anisotropic (discussed later), strong vortex dynamics suppresses J in the measured time window. In other words, J_c can be larger at even lower temperatures, or if we measure it in a much shorter time scale. Another possibility is that the material may have a stacking fault due to the large Pt deficiency in the Pt-As layer. In this case, J_c would also be strongly suppressed.

The temperature dependence of reduced J_c of $Ca_{10}(Pt_{4-\delta}As_8)(Fe_{2-x}Pt_xAs_2)_5$ under zero field is shown in Fig. 3(b). The temperature dependence of J_c is well approximated by $J_c(T) = J_c(0)\exp(-T/T_0)$ with $T_0 \approx 3.9$ K, where $J_c(0)$ is the critical current density at zero temperature under zero field and T_0 is a characteristic temperature for vortex creep. The exponential temperature dependence arises from nonlinear effective flux-creep activation energy due to weak collective pinning of magnetic flux lines.[41–43] For comparison, the temperature dependence of normalized J_c of $Ba(Fe_{0.93}Co_{0.07})_2As_2$ extracted from Ref. 25 is also plotted in this figure. As is evident, the $Ca_{10}(Pt_{4-\delta}As_8)(Fe_{2-x}Pt_xAs_2)_5$ behaves like most widely studied iron-based superconductor $Ba(Fe_{1-x}Co_x)_2As_2$, but has stronger temperature dependence. This $J_c(T)$ behavior of $Ca_{10}(Pt_{4-\delta}As_8)(Fe_{2-x}Pt_xAs_2)_5$ is also similar to that of $YBa_2Cu_3O_{7-\delta}$ (Refs. 44 and 45). In general, T_0 is strongly correlated with the anisotropy of the superconducting materials. The smaller T_0 corresponds to a larger anisotropy for superconductors with similar T_c. $T_0 = 3.9$ K in $Ca_{10}(Pt_{4-\delta}As_8)(Fe_{2-x}Pt_xAs_2)_5$ is smaller than $T_0 = 11.5$ K in $Ba(Fe_{0.93}Co_{0.07})_2As_2$, indicating that the anisotropy in this superconductor is larger than that in $Ba(Fe_{0.93}Co_{0.07})_2As_2$. Actually, as estimated later, the anisotropy of $Ca_{10}(Pt_{4-\delta}As_8)(Fe_{2-x}Pt_xAs_2)_5$ is much larger than that of $Ba(Fe_{0.93}Co_{0.07})_2As_2$, and close to that of $La_{2-x}Sr_xCuO_{4-\delta}$ (Ref. 46).

The above estimate of J_c relies on the assumption that the homogeneous current is flowing within the sample. To examine this assumption, we made MO imaging of a 19-μm thick $Ca_{10}(Pt_{4-\delta}As_8)(Fe_{2-x}Pt_xAs_2)_5$ single crystal in the remnant state at several temperatures ranging from 5 to 25 K. The remnant state is prepared by applying 800 Oe along the c axis for 1 s and removing it after zero-field cooling. Figures 4(a)–4(c) show MO images of $Ca_{10}(Pt_{4-\delta}As_8)(Fe_{2-x}Pt_xAs_2)_5$ in the remnant state at 5, 10, and 15 K, respectively. Figure 4(d) shows profiles of the magnetic induction at different temperatures along the line shown in Fig. 4(a). At lower temperatures, the MO image shows a nearly uniform current flow in the sample. J_c for a thin superconductor is roughly estimated by

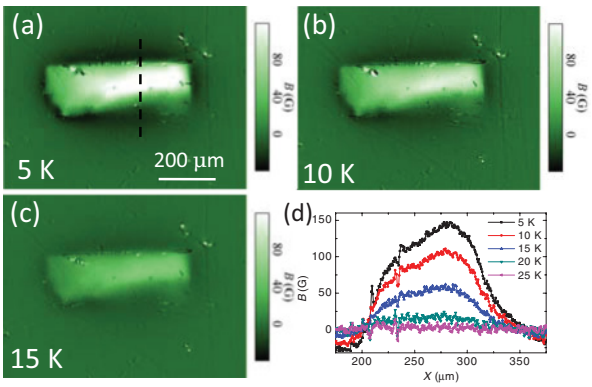

FIG. 4. (Color online) (a) Magneto-optical images in the remnant state after applying 800 Oe in $Ca_{10}(Pt_{4-\delta}As_8)(Fe_{2-x}Pt_xAs_2)_5$ at 5, 10, and 15 K. (d) The local magnetic induction profiles at different temperatures taken along the dashed lines in (a).

$J_c \sim \Delta B/t$, where ΔB is the trapped field and t is the thickness of the sample. With $\Delta B \sim 150$ G and $t = 19$ μm, J_c is estimated as $\sim 0.8 \times 10^5$ A/cm^2 at 5 K, which is in good agreement with the value obtained from the M-H curve.

The variations of T_c with magnetic field from 0 to 50 kOe for $H \| c$ and $H \| ab$ are shown in Figs. 5(a) and 5(b), respectively. With increasing field, the resistive transition shifts to lower temperatures accompanied by an increase in the transition width, especially for $H \| c$, which also indicates the presence of the strong thermal fluctuation of the vortices. The broadening is almost negligible for $H \| ab$. With the 50-kOe field, the T_c was suppressed to $0.76T_{c0}$ for $H \| c$ and $0.94T_{c0}$ for $H \| ab$, where T_{c0} is the transition temperature under zero field.

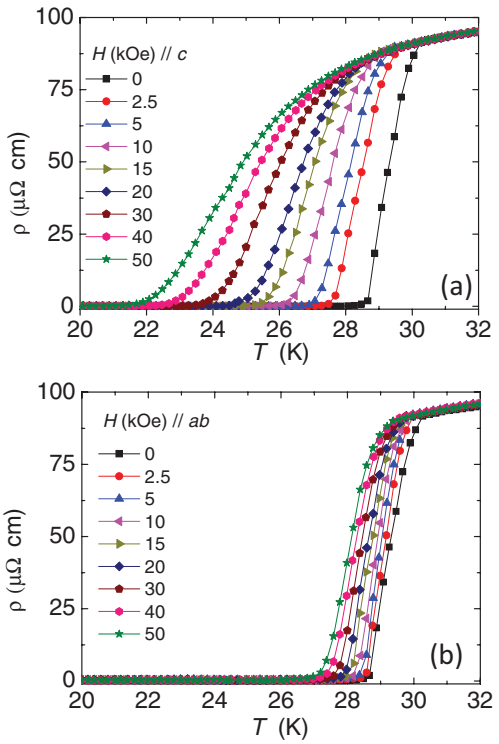

FIG. 5. (Color online) Magnetic field dependence of in-plane resistivity for (a) $H \| c$ and (b) $H \| ab$.

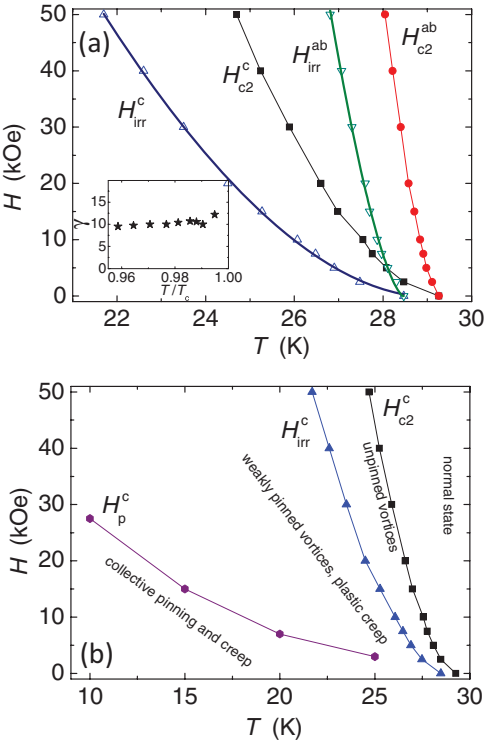

FIG. 6. (Color online) (a) Temperature dependence of upper critical field and irreversible field for $H \| c$ and $H \| ab$ obtained by the 50% and 1% of normal state resistivity in $Ca_{10}(Pt_{4-\delta}As_8)(Fe_{2-x}Pt_xAs_2)_5$. The solid lines are fits to $H^{ab}_{irr}(T) \approx (1 - T/T_c)^{1.50}$ and $H^c_{irr}(T) \approx (1 - T/T_c)^{1.75}$. The inset shows the anisotopic parameter $\gamma(T) = H^{ab}_{c2}/H^c_{c2}$. (b) The H-T phase diagram for $H \| c$ of $Ca_{10}(Pt_{4-\delta}As_8)(Fe_{2-x}Pt_xAs_2)_5$ single crystals in the mixed state.

Figure 6(a) shows the variation of the upper critical field H_{c2} and irreversibility field H_{irr} with the temperature for $Ca_{10}(Pt_{4-\delta}As_8)(Fe_{2-x}Pt_xAs_2)_5$. The values of H_{c2} are defined as the field at the midpoint of the resistive transition. The slopes of H_{c2} are -16.8 and -57.1 kOe/K along the c and ab directions, respectively, extracted from the linear part between 30 and 50 kOe. From the Werthamer-Helfand-Hohenberg theory,[47] which describes the orbital depairing field for conventional dirty type II superconductors, the value of H_{c2} at $T = 0$ K is estimated using $H_{c2}(0) = 0.69T_c|dH_{c2}/dT|_{T=T_c}$. $H^c_{c2}(0)$ and $H^{ab}_{c2}(0)$ are estimated as 339 and 1,154 kOe, respectively. The anisotropy parameter $\gamma = H^{ab}_{c2}/H^c_{c2} = \sqrt{m^*_c/m^*_{ab}}$ shown in the inset is around 10 near T_{c0}. The anisotropy of $Ca_{10}(Pt_{4-\delta}As_8)(Fe_{2-x}Pt_xAs_2)_5$ is much larger than the typical value around 2∼3 in $Ba(Fe_{0.93}Co_{0.07})_2As_2$ (Ref. 25). This is consistent with the tendency inferred from the temperature dependence of the critical current density measurement. The anisotropy of our sample is also larger than that in Ref. 21, the higher T_c of our sample may be the reason for this difference.

The large anisotropy together with the broadening of the superconducting transition under magnetic field suggests the existence of a wide vortex-liquid phase when the magnetic field is applied along the c axis. The $Ca_{10}(Pt_{4-\delta}As_8)(Fe_{2-x}Pt_xAs_2)_5$ crystal is not the only superconductor in iron-based superconductors having a relatively large anisotropy. For example, 1111 also shows large anisotropy.[48] There have been several

reports showing the presence of a reversible region, which corresponds to the vortex liquid phase in the global sense.[48–50] In this sense, the separation of H_{irr} and H_{c2} is evidence for the presence of the vortex liquid phase. However, no vortex solid to liquid transitions accompanying a clear first-order signature of the transition have been reported.[51,52]

To extract the superconducting parameters we have used the Ginzburg-Landau (GL) formula for the coherence length (ξ). ξ is calculated from the estimated $H_{c2}(0)$'s data using the relations given by $H_{c2}^{ab}(0) = \Phi_0/2\pi\xi_{ab}\xi_c, H_{c2}^{c}(0) = \Phi_0/2\pi\xi_{ab}^2$,where $\Phi_0 = 2.07 \times 10^{-7}$ G cm^2, the obtained $\xi_{ab} \sim 1.74$ nm and $\xi_c \sim 5.92$ nm. The values of H_{irr} were defined as the field at 1% of the normal state resistivity. The temperature dependence of the irreversibility field is well approximated by $H_{irr}^{ab}(T) \approx (1 - T/T_c)^{1.50}$ and $H_{irr}^{c}(T) \approx (1 - T/T_c)^{1.75}$. Such a $(1-T/T_c)^n$-type temperature dependence of H_{irr} can be explained by using a thermally activated flux creep model.[37] The power exponent 1.50 for $H_{irr}^{ab}(T)$ of $Ca_{10}(Pt_{4-\delta}As_8)(Fe_{2-x}Pt_xAs_2)_5$ is close to that of $YBa_2Cu_3O_{7-\delta}$ (Ref. 53) and $Ba(Fe_{0.93}Co_{0.07})_2As_2$ (Ref. 54).

Adopting similar analyses to those in Ref. 30, the phase diagram of the $Ca_{10}(Pt_{4-\delta}As_8)(Fe_{2-x}Pt_xAs_2)_5$ single crystals in the mixed state is plotted in Fig. 6(b). Here H_p is the magnetic field of the peak position in the M-H curve. This phase diagram is also similar to that of $Ba(Fe_{1-x}Co_x)_2As_2$ (Refs. 39 and 54), $Ba_{1-x}K_xFe_2As_2$ (Ref. 55), and high-T_c cuprates.

IV. CONCLUSION

In conclusion, x-ray diffraction, magnetization, resistivity, and magneto-optical measurements were performed on high quality $Ca_{10}(Pt_{4-\delta}As_8)(Fe_{2-x}Pt_xAs_2)_5$ single crystals. Magnetooptical imaging revealed a nearly homogeneous current flow in the crystal. The magnetization measurements reveal a fish-tail hysteresis loop in the intermediate temperature range. The value of J_c is over 0.8×10^5 A/cm^2 below 5 K under zero field, which is promising for practical applications. Upper critical fields obtained by resistive transition are 339 and 1,154 kOe at zero temperature along the c and ab directions, respectively. The anisotropy parameter γ near T_c is around 10. The temperature dependence of J_c also suggests that the anisotropy in $Ca_{10}(Pt_{4-\delta}As_8)(Fe_{2-x}Pt_xAs_2)_5$ is much larger than that of $Ba(Fe_{0.93}Co_{0.07})_2As_2$.

[1] Y. Kamihara, T. Watanabe, M. Hirano, and H. Hosono, J. Am. Chem. Soc. **130**, 3296 (2008).
[2] G. F. Chen, Z. Li, D. Wu, G. Li, W. Z. Hu, J. Dong, P. Zheng, J. L. Luo, and N. L. Wang, Phys. Rev. Lett. **100**, 247002 (2008).
[3] P. Cheng, L. Fang, H. Yang, X. Y. Zhu, G. Mu, H. Q. Luo, Z. S. Wang, and H. H. Wen, Sci. China Ser. G **51**, 719 (2008).
[4] Z. A. Ren, G. C. Che, X. L. Dong, J. Yang, W. Lu, W. Yi, X. L. Shen, Z. C. Li, L. L. Sun, F. Zhou, and Z. X. Zhao, Europhys. Lett. **83**, 17002 (2008).
[5] J. H. Tapp, Z. Tang, B. Lv, K. Sasmal, B. Lorenz, P. C. W. Chu, and A. M. Guloy, Phys. Rev. B **78**, 060505(R) (2008).
[6] S. Matsuishi, Y. Inoue, T. Nomura, H. Yanagi, M. Hirano, and H. Hosono, J. Am. Chem. Soc. **130**, 14428 (2008).
[7] X. Zhu, F. Han, G. Mu, B. Zeng, P. Cheng, B. Shen, and H.-H. Wen, Phys. Rev. B **79**, 024516 (2009).
[8] M. Rotter, M. Tegel, and D. Johrendt, Phys. Rev. Lett. **101**, 107006 (2008).
[9] X. C. Wang, Q. Q. Liu, Y. X. Lv, W. B. Gao, L. X. Yang, R. C. Yu, F. Y. Li, and C. Q. Jin, Solid State Commun. **148**, 538 (2008).
[10] F. C. Hsu, J. Y. Luo, K. W. Yeh, T. K. Chen, T. W. Huang, P. M. Wu, Y. C. Lee, Y. L. Huang, Y. Y. Chu, D. C. Yan, and M. K. Wu, Proc. Natl. Acad. Sci. **105**, 14262 (2008).
[11] X. Zhu, F. Han, G. Mu, P. Cheng, B. Shen, B. Zeng, and H.-H. Wen, Phys. Rev. B **79**, 220512(R) (2009).
[12] H. Ogino, Y. Katsura, S. Horii, K. Kishio, and J. Shimoyama, Supercond. Sci. Technol. **22**, 085001 (2009).
[13] Y. Matsumura, H. Ogino, S. Horii, Y. Katsura, K. Kishio, and J. Shimoyama, Appl. Phys. Express **2**, 063007 (2009).
[14] N. Kawaguchi, H. Ogino, Y. Shimizu, K. Kishio, and J. Shimoyama, Appl. Phys. Express **3**, 063102 (2010).
[15] H. Ogino, K. Machida, A. Yamamoto, K. Kishio, J. Shimoyama, T. Tohei, and Y. Ikuhara, Supercond. Sci. Technol. **23**, 115005 (2010).
[16] S. Sato, H. Ogino, N. Kawaguchi, Y. Katsura, K. Kishio, J. Shimoyama, H. Kotegawa, and H. Tou, Supercond. Sci. Technol. **23**, 045001 (2010).
[17] P. M. Shirage, K. Kihou, C.-H. Lee, H. Kito, H. Eisaki, and A. Iyo, Appl. Phys. Lett. **97**, 172506 (2010).
[18] H. Ogino, S. Sato, K. Kishio, J. Shimoyama, T. Tohei, and Y. Ikuhara, Appl. Phys. Lett. **97**, 072506 (2010).
[19] K. Kudo, International workshop on novel superconductors and super materials, Tokyo, Japan, March 6–8 (2011).
[20] S. Kakiya, K. Kudo, Y. Nishikubo, K. Oku, E. Nishibori, H. Sawa, T. Yamamoto, T. Nozaka, and M. Nohara, J. Phys. Soc. Jpn. **80**, 093704 (2011).
[21] N. Ni, J. M. Allred, B. C. Chan, and R. J. Cava, Proc. Natl. Acad. Sci **108**, E1019 (2011).
[22] C. Lohnert, T. Sturzer, M. Tegel, R. Frankovsky, G. Friederichs, and D. Hohrendt, Angew. Chem. Int. Ed. **50**, 9195 (2011).
[23] K. Cho, M. A. Tanatar, H. Kim, W. E. Straszheim, N. Ni, R. J. Cava, and R. Prozorov, Phys. Rev. B **85**, 020504(R) (2012).
[24] M. Fang, J. Yang, F. F. Balakirev, Y. Kohama, J. Singleton, B. Qian, Z. Q. Mao, H. Wang, and H. Q. Yuan, Phys. Rev. B **81**, 020509(R) (2010).
[25] Y. Nakajima, T. Taen, and T. Tamegai, J. Phys. Soc. Jpn. **78**, 023702 (2009).
[26] M. Kano, Y. Kohama, D. Graf, F. Blakirev, A. S. Sefat, M A. Mcguire, B. C. Sales, D. Mandrus, and S. W. Tozer, J. Phys. Soc. Jpn. **78**, 084719 (2009).
[27] A. Soibel, E. Zeldov, M. Rappaport, Y. Myasoedov, T. Tamegai, O. Ooi, M. Konczykowski, and V. B. Geshkenbein, Nature (London) **406**, 282 (2000).
[28] M. Yasugaki, K. Itaka, M. Tokunaga, N. Kameda, and T. Tamegai, Phys. Rev. B **65**, 212502 (2002).
[29] C. P. Bean, Rev. Mod. Phys. **36**, 31 (1964).

[30]M. Daumling, J. M. Seuntjens, and D. C. Larbalestier, Nature (London) **346**, 332 (1990).
[31]Y. Radzyner, A. Shaulov, Y. Yeshurun, I. Felner, K. Kishio, and J. Shimoyama, Phys. Rev. B **65**, 214525 (2002).
[32]T. Tamegai, Y. Iye, I. Oguro, and K. Kishio, Physica C **213**, 33 (1993).
[33]C. J. van der Beek, M. Konczykowski, S. Kasahara, T. Terashima, R. Okazaki, T. Shibauchi, and Y. Matsuda, Phys. Rev. Lett. **105**, 267002 (2010).
[34]L. Fang, Y. Jia, J. A. Schlueter, A. Kayani, Z. L. Xiao, H. Claus, U. Welp, A. E. Koshelev, G. W. Crabtree, and W.-K. Kwok, Phys. Rev. B **84**, 140504(R) (2011).
[35]A. B. Pippard, Philosophical Magazine **19**, 217 (1969).
[36]O. Daldini, P. Martinoli, J. L. Olsen, and G. Berner, Phys. Rev. Lett. **32**, 218 (1974).
[37]G. Blatter, M. V. Feigel'man, V. B. Geshkenbein, A. I. Larkin, and V. M. Vinokur, Rev. Mod. Phys. **66**, 1125 (1994).
[38]L. Krusin-Elbaum, L. Civale, V. M. Vinokur, and F. Holtzberg, Phys. Rev. Lett. **69**, 2280 (1992).
[39]R. Prozorov, N. Ni, M. A. Tanatar, V. G. Kogan, R. T. Gordon,C. Martin, E. C. Blomberg, P. Prommapan, J. Q. Yan, S. L. Bud'ko, and P. C. Canfield, Phys. Rev. B **78**, 224506 (2008).
[40]T. Taen, Y. Tsuchiya, Y. Nakajima, and T. Tamegai, Phys. Rev. B **80**, 092502 (2009).
[41]J. R. Thompson, Y. R. Sun, L. Civale, A. P. Malozemoff, M. W. McElfresh, A. D. Marwick, and F. Holtzberg, Phys. Rev. B **47**, 14440 (1993).
[42]M. Paranthaman, J. R. Thompson, Y. R. Sun, and J. Brynestad, Physica C **213**, 271 (1993).
[43]D. K. Christen and J. R. Thompson, Nature (London) **364**, 98 (1993).
[44]P. H. Kes, Physica C **153-155**, 1121 (1988).
[45]T. Tamegai, L. Krusin-Elbaum, P. Santhanam, M. J. Brady, W. T. Masselink, C. Feild, and F. Holtzberg, Phys. Rev. B **45**, 2589(R) (1992).
[46]Y. Radzyner, A. Shaulov, Y. Yeshurun, I. Felner, K. Kishio, and J. Shimoyama, Phys. Rev. B **65**, 214525 (2002).
[47]N. R. Werthamer, E. Helfand, and P. C. Hohenberg, Phys. Rev. **147**, 295 (1966).
[48]J. Kacmarcik, C. Marcenat, T. Klein, Z. Pribulova, C. J. van der Beek, M. Konczykowski, S. L. Budko, M. Tillman, N. Ni, and P. C. Canfield, Phys. Rev. B **80**, 014515 (2009).
[49]Z. Pribulova, T. Klein, J. Kacmarcik, C. Marcenat, M. Konczykowski, S. L. Budko, M. Tillman, and P. C. Canfield, Phys. Rev. B **79**, 020508 (2009).
[50]G. Prando, P. Carretta, R. De Renzi, S. Sanna, A. Palenzona, M. Putti, and M. Tropeano, Phys. Rev. B **83**, 174514 (2011).
[51]Zeldov, D. Majer, M. Konczykowski, V. B. Geshkenbein, V. M. Vinokur, and H. Shtrikman, Nature (London) **375**, 373 (1995).
[52]A. Schilling, R. A. Fisher, N. E. Phillips, U. Welp, D. Dasgupta, W. K. Kwok, and G. W. Crabtree, Nature (London) **382**, 791 (1996).
[53]Y. Yeshurun and A. P. Malozemoff, Phys. Rev. Lett **60**, 2202 (1988).
[54]B. Shen, P. Cheng, Z. S. Wang, L. Fang, C. Ren, L. Shan, and H.-H. Wen, Phys. Rev. B **81**, 014503 (2010).
[55]S. Salem-Sugui Jr., L. Ghivelder, A. D. Alvarenga, L. F. Cohen, K. A. Yates, K. Morrison, J. L. Pimentel Jr., H. Luo, Z. Wang, and H.-H. Wen, Phys. Rev. B **82**, 054513 (2010).